A Theoretical Investigation of the Low Lying Electronic Structure of Poly(p-phenylene vinylene).

Mikhail Yu. Lavrentiev[1*], William Barford[1], Simon J. Martin[1], Helen Daly[1] and Robert J. Bursill[2]

[1]Department of Physics and Astronomy, The University of Sheffield, Sheffield, S3 7RH, United Kingdom

[2]School of Physics, University of New South Wales, Sydney, NSW 2052, Australia

Abstract

The two-state molecular orbital model of the one-dimensional phenyl-based semiconductors is applied to poly(*para*-phenylene vinylene). The energies of the low-lying excited states are calculated using the density matrix renormalization group method. Calculations of both the exciton size and the charge gap show that there are both $^1B_u^-$ and $^1A_g^+$ excitonic levels below the band threshold. The energy of the $1^1B_u^-$ exciton extrapolates to 2.60 eV in the limit of infinite polymers, while the energy of the $2^1A_g^+$ exciton extrapolates to 2.94 eV. The calculated binding energy of the $1^1B_u^-$ exciton is 0.9 eV for a 13 phenylene unit chain and 0.6 eV for an infinite polymer. This is expected to decrease due to solvation effects. The lowest triplet state is calculated to be at ca. 1.6 eV, with the triplet-triplet gap being ca. 1.6 eV. A comparison between theory, and two-photon absorption and electroabsorption is made, leading to a consistent picture of the essential states responsible for most of the third-order nonlinear optical properties. An interpretation of the experimental nonlinear optical spectroscopies suggests an energy difference of ca. 0.4 eV between the vertical energy and ca. 0.8 eV between the relaxed energy, of the $1^1B_u^-$ exciton and the band gap, respectively.

1 Introduction

Since the discovery of the electro-luminescent properties of the organic semiconductor poly(para-phenylene vinylene) (PPV) [1] an understanding of its low lying electronic structure has remained a challenge. The observation of electroluminescence implies that there is a one-photon transition from the lowest excited singlet state to the ground state. The structure of PPV, a sequence of phenylene and vinylene units capped by phenyl rings, is shown in Fig. 1. Since PPV is centro-symmetric, and thus possess C_2 symmetry, the ground state is spatially symmetric (A_g), while the first excited singlet state is therefore odd under rotation (B_u). Furthermore, PPV, to a very good approximation, is non-polar (i.e. each atom is charge neutral) and thus another symmetry it possesses is particle-hole symmetry. As one-photon transitions occur between states of opposite particle-hole symmetry, we will confine out attention to the A_g^+ and B_u^- symmetry sectors in this paper.

Figure 1: Poly(para phenylene vinylene). $N = 0$ corresponds to stilbene.

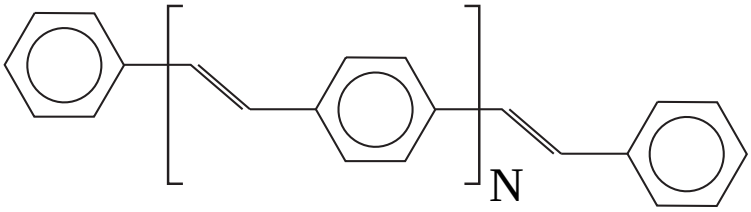

A number of optical probes have been employed to ascertain the character of the low lying states. In particular, one-photon absorption identifies the ${}^1B_u^-$ states, two-photon absorption (TPA) identifies the ${}^1A_g^+$ states, and electroabsorption (EA) and third harmonic generation (THG) identify both kinds of states. A consistent picture of the low lying electronic structure of PPV has been slow to emerge, owing to sample variability (including the use of PPV derivatives), inter-chain effects, and the fact that some measurements probe vertical transitions, while others probe relaxed transitions. Nonetheless, a consistent experimental interpretation is beginning to appear, and we discuss and interpret current experiments in the light of our and other theoretical calculations.

A full theoretical treatment must include the effects of the strong electron-electron interactions, electron-lattice relaxation and inter-chain interactions to fully describe PPV thin films. So far, however, most calculations have considered single chains in the absence of electron-lattice relaxation. Furthermore, they have included electron-electron interactions in the most simple way, e.g., by Hartree-Fock mean field or by the single configuration interaction (SCI), neither of which can describe the highly correlated ${}^1A_g^+$ states of conjugated semiconductors.

A remarkably reliable description of π conjugated electron systems is provided by the semi-empirical one band Pariser-Parr-Pople (P-P-P) model. Both Shimoi and Abe [2], and Chandross and Mazumdar [3] solved a re-parametrised P-P-P model, within the SCI approximation, to obtain the optical transitions and conduction band edge. Shimoi and Abe predicted a $1^1B_u^-$ exciton at 2.4 eV and the band edge at 3.2 eV, while Chandross and Mazumdar obtained results of 2.7 eV and 3.6 eV for the $1^1B_u^-$ exciton and band edge, respectively. Gomes da Costa and Conwell [4] used as their model of PPV thin films the physics of three dimensional semiconductors and Wannier excitons. Using a phenomenological dielectric constant they obtained the $1^1B_u^-$ exciton at 2.4 eV and the band gap at 2.8 eV. Rice and Gartstein [5] presented a phenomenological model based on the molecular orbitals which was solved analytically. They predicted a binding energy of ca. 0.1 eV. In a later paper [6], a more elaborate model was presented, with a binding energy lying between 0.2 and 0.4 eV. Beljonne et al. [7] performed a INDO/MRD-CI study of PPV oligomers in a molecular model. By extrapolating to an eight phenylene ring oligomer, they associate the onset of the conduction band by the $n^1B_u^-$ state at 4.73 eV, and locate other important states below it: $1^1B_u^-$ at 3.13 eV, $2^1A_g^+$ at 3.78 eV, and $m^1A_g^+$ at 4.28 and 4.73 eV. Thus, their

results suggest that these states are essentially excitonic. Harigaya [8] performed a single-CI study of PPV, poly(p-phenylene) (PPP) and related polymers. In particular, for PPV he found the Hartree-Fock gap at 3.64 eV and the onset of long-range excitons at only a slightly lower energy of 3.60 eV.

In this paper we employ the two-state molecular orbital (MO) model introduced in [9] and [10] to calculate the energies and correlation functions of the low lying, predominately long axis polarised, states of single oligomers. The model and its parametrisation is discussed in §2. In this treatment we also neglect electron-lattice relaxation and inter-chain effects. However, since the model is solved by the density matrix renormalisation group (DMRG) method [11], an essentially exact treatment of one dimensional quantum Hamiltonians, electron-electron correlations are correctly treated. As discussed in §3, we predict bands of B_u^- and A_g^+ excitons. We identify the onset of the unbound states by an examination of the particle-hole correlation function. We further show that the first unbound ${}^1A_g^+$ state couples strongly to the $1^1B_u^-$ exciton, and hence contributes to the EA spectrum. In §4 the TPA and EA spectra of oligophenylene-vinylenes are calculated. By comparing the calculated and experimental TPA and EA spectra, we deduce a coherent picture of the energies and symmetries of the low lying states. We conclude in §5.

2 The Two State Model

The essential assumption underlying the two-state MO model is that the six MOs of the phenyl(ene) ring, arising from the six conjugated π electrons, may be replaced by the bonding HOMO and LUMO states. In principle, the many body correlations between the MOs can be determined from the underlying P-P-P model. When this was done for PPP, however, it was found that there is a poor agreement with experiment [12]. This is a result of the neglect of the many body correlations involving the neglected orbitals. Nevertheless, if a description of the low energy predominately long-axis polarised states is required, a two-state model should contain the essential physics. (The meaning of a predominately long-axis polarised state will be discussed shortly.) Thus the two-state model is a *phenomenological* model whose parameters are chosen to agree with exact P-P-P model calculations of benzene, biphenyl and stilbene. This approach was adopted for PPP in [10], and where comparison to experiment could be made, was found to be succesful. We will show that its application to PPV also leads to a consistent agreement with experiment. The transformation from atomic to molecular orbitals is performed for phenyl(ene) and vinylene units, and below we denote the HOMO orbital by $|1\rangle$ and the LUMO by $|2\rangle$ for both types of molecular units.

The 2-MO model reads,

$$H = -\sum_{i\,\alpha\,\beta\,\sigma} t_{\alpha\beta}\left[a^\dagger_{i\alpha\sigma}a_{i+1\beta\sigma} + \text{h.c.}\right] + \sum_{i\,\alpha}\epsilon_\alpha(n_{i\alpha}-1) + U\sum_{i\,\alpha}\left(n_{i\alpha\uparrow}-\frac{1}{2}\right)\left(n_{i\alpha\downarrow}-\frac{1}{2}\right)$$

$$+\frac{U}{2}\sum_{i\,\alpha\neq\beta}(n_{i\alpha}-1)(n_{i\beta}-1)+V\sum_{i\,\alpha\,\beta}(n_{i\alpha}-1)(n_{i+1\beta}-1)$$
$$-X\sum_{i\,\alpha\neq\beta}\left[\boldsymbol{S}_{i\alpha}.\boldsymbol{S}_{i\beta}+\frac{1}{4}\left(n_{i\alpha}-1\right)\left(n_{i\beta}-1\right)\right]$$
$$+\frac{P}{2}\sum_{i\,\alpha\neq\beta\,\sigma}a^{\dagger}_{i\alpha\sigma}a^{\dagger}_{i\alpha\bar{\sigma}}a_{i\beta\bar{\sigma}}a_{i\beta\sigma}, \qquad (1)$$

where $a^{\dagger}_{i\alpha\sigma}$ creates an electron in the molecular orbital α on the molecular repeat unit i with the spin σ; $\boldsymbol{S}_{i\alpha}=\sum_{\rho\rho'}a^{\dagger}_{i\alpha\rho}\boldsymbol{\sigma}_{\rho\rho'}a_{i\alpha\rho'}$ and $\boldsymbol{\sigma}$ are the Pauli spin matrices. The creation of an exciton in this model corresponds to the excitation of an electron from a HOMO to a LUMO state on the same or a near by unit, resulting in a bound electron-hole pair.

The intra-phenyl(ene) parameters were derived in [10] by comparing to P-P-P model calculations of benzene and biphenyl [13]. Since the vinylene unit is exactly described by its HOMO and LUMO states, its intra-unit interactions are found by an exact mapping from the atomic orbital basis of the P-P-P model to the MO basis. The P-P-P model parameters are those derived in [13]. The remaining parameters are the inter-unit Coulomb repulsion, V and the inter-unit hybridisation, t. We will assume that $V=(U_{phenylene}+U_{vinylene})/4$. Finally, t is parametrised by fitting the 2-MO model prediction of the $1^1B_u^-$ exciton in stilbene to a P-P-P model calculation, which puts it at 4.17 eV [14] (in excellent agreement with experiment). The parameters are summarised in Table 1.

Parameter	Phenyl(ene) unit	Vinylene unit
Intra-unit HOMO-LUMO gap	5.26	5.43
Intra-unit Coulomb repulsion	3.67	8.70
Inter-unit Coulomb repulsion	3.09	3.09
Intra-unit exchange energy	0.89	1.36
Intra-unit pair hopping	0.89	1.36
Inter-unit hybridisation	1.27	1.27

Table 1: Parameters used in the 2-MO model (eV).

We can use the P-P-P model calculation of stilbene to evaluate the success of the 2-MO model for other states. Before doing that we need to discuss the effect of long range Coulomb correlations on the spatial symmetry of the electronic states. In the absence of Coulomb interactions the P-P-P Hamiltonian of stilbene (and PPV) possess topological D_{2h} symmetry. The irreducible representation of the D_{2h} group are A_g (symmetric), B_{1u} (long-axis polarised), B_{2u} (short axis-polarised) and B_{3g} (anti-symmetric). The effect of the Coulomb interactions is to weakly break the topological D_{2h} symmetry and render the molecule C_2 symmetric. Thus, the electronic states

evolve from A_g and B_{3g} to A_g, and B_{1u} and B_{2u} to B_u. Nevertheless, the dipole active states are either *predominately* long-axis or short-axis polarised. Now, the 2-MO model describes B_u states which are predominately long-axis polarised (i.e. B_{1u} states in the absence of symmetry breaking terms) and A_g states which would be A_g (and not B_{3g}) in the absence of symmetry breaking terms. The relevant lowest excited A_g state of stilbene to compare with the 2-MO model prediction is at 5.18 eV [15]. The 2-MO model value of 5.24 eV has a relative error of 1.3 %. Similarly, the P-P-P model value of 2.77 eV for the $1^3B_u^+$ state compares well with the 2-MO model prediction of 2.65 eV (a relative error of -4.2 %).

The calculations of the energies of the ground and lowest excited states, as well as their properties are performed using the DMRG method [11]. The details of the implementation of the method are given in [10], together with results of numerous accuracy tests.

3 The low energy spectra and correlation functions

3.1 The Singlet Spectrum

Fig. 2 (a) shows the energy spectra of the key low lying $^1B_u^-$ states as a function of oligomer length. The energy of the lowest $^1B_u^-$ state extrapolates to 2.60 eV in the limit of infinite polymers. The experimental oligomer vertical energies of the $1^1B_u^-$ exciton, obtained from one-photon absorption [16], are plotted in Fig. 2(a). These are in excellent agreement with our calculation. The typical PPV thin film result of ca. 2.8 eV for the vertical transition [17] is also in close agreement with the infinite polymer result of 2.60 eV. Note that the $0-0$ transition is typically 2.4 eV [17]. The low lying $^1A_g^+$ spectrum is shown in Fig. 2(b). The energy of the first excited $^1A_g^+$ state ($2^1A_g^+$) extrapolates to 2.94 eV.

To distinguish between bound (i.e. exciton) and unbound (i.e. band) states, the spatial correlation function [10], defined as

$$C_{ij}(|n\rangle) = \langle n| \, S_{ij}^\dagger \left|1^1A_g^+\right\rangle, \tag{2}$$

is calculated. Here, $S_{ij}^\dagger$ is a singlet exciton creation operator, which removes a particle from the HOMO on repeat unit j and places it into the LUMO on repeat unit i:

$$S_{ij}^\dagger = \frac{1}{\sqrt{2}}(a_{i2\uparrow}^\dagger a_{j1\uparrow} + a_{i2\downarrow}^\dagger a_{j1\downarrow}) \tag{3}$$

This correlation function is used to calculate the mean particle-hole spacing, as shown in Fig. 3. The particle-hole separation of the $1^1B_u^-$ and $2^1A_g^+$ excitons are roughly one and two to three phenylene-vinylene repeat units, respectively. The $^1B_u^-$ excitons are more tightly bound than the $^1A_g^+$ excitons, because the former, being negative under the particle-hole operator, are 's'-wave excitons, while the latter, being positive under the particle-hole operator, are 'p'-wave excitons [10].

Figure 2: (a) The energies of the key lowest bound and band states of ${}^1B_u^-$ symmetry, and the charge gap, E_G, as a function of the number of phenylene units. $1{}^1B_u^-$ (solid diamonds), $2{}^1B_u^-$ (solid triangles), $3{}^1B_u^-$ (solid squares), $n{}^1B_u^-$ (open diamonds), and E_G (dashed line). The experimental results are shown as crosses [16]. (b) The energies of the key lowest bound and band states of ${}^1A_g^+$ symmetry, and the charge gap, E_G, as a function of the number of phenylene units. $2{}^1A_g^+$ (solid squares), $3{}^1A_g^+$ (solid diamonds), $4{}^1A_g^+$ (solid triangles), $m{}^1A_g^+$ (open squares), and E_G (dashed line).

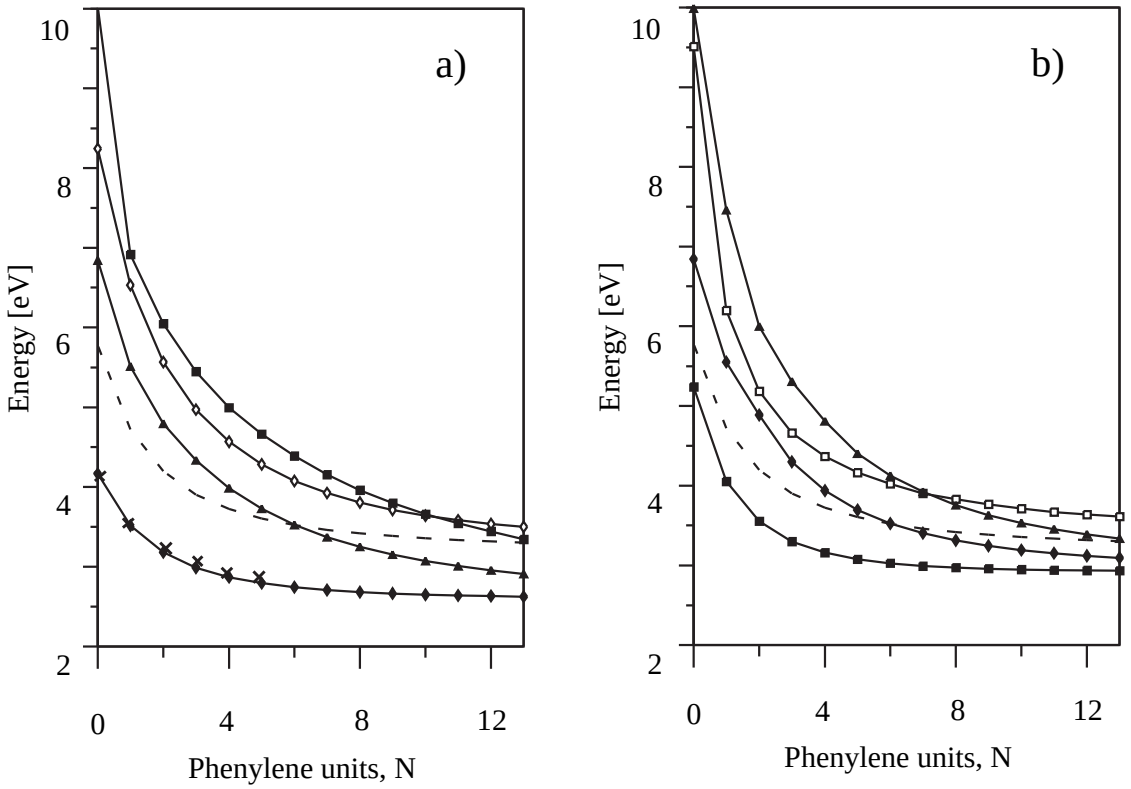

Figure 3: The mean electron-hole distance of the key lowest bound and band states as a function of the number of phenylene units. $1^1B_u^-$ (solid diamonds), $2^1A_g^+$ (solid squares), $n^1B_u^-$ (open diamonds), and $m^1A_g^+$ (open squares).

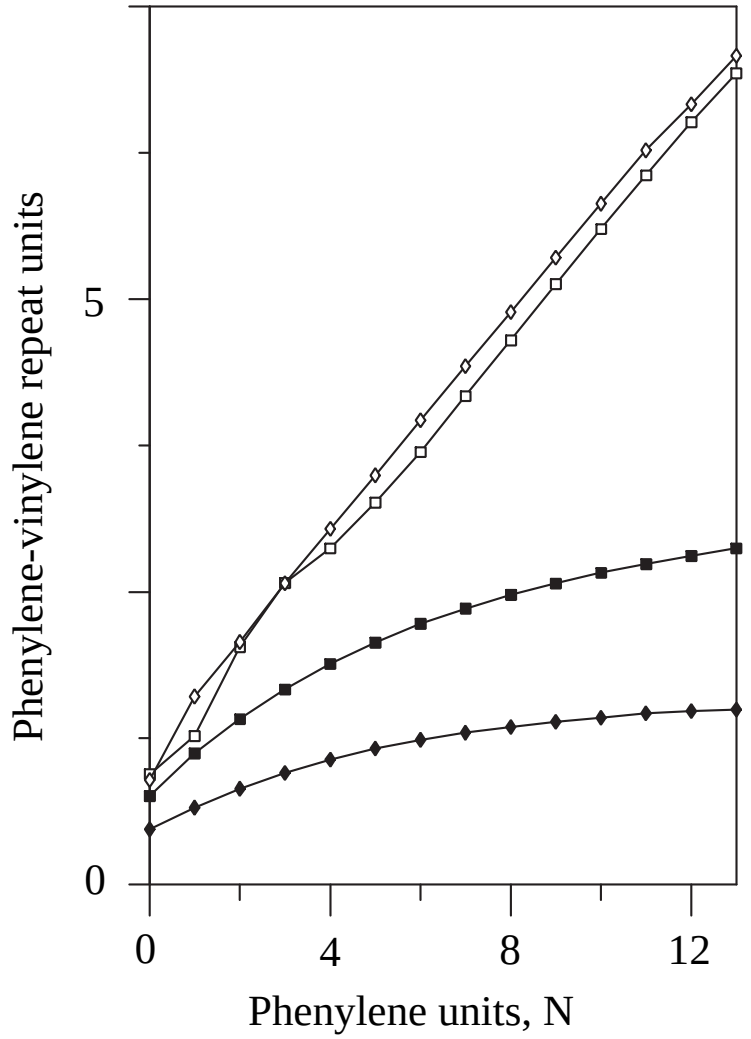

Also shown in Fig. 3 are the lowest two unbound states, with an average spacing increasing linearly with oligomer length. The first unbound state in the $^1A_g^+$ symmetry sector is denoted by $m^1A_g^+$, where $m = 7$ for oligomers of 10 to 13 phenylene units. As shown in the next section, this is the state with the largest dipole moment with the excitonic $1^1B_u^-$ state, and thus will contribute to the non-linear optical spectroscopies [18]. In the $^1B_u^-$ sector we denote the first unbound state as the $n^1B_u^-$ state, where $n = 4$ for a 13 phenylene unit oligomer.

The energies of the $n^1B_u^-$ and $m^1A_g^+$ states, which extrapolate to ca. 3.2 eV for infinite polymers, are shown in Fig. 2 (a) and (b), respectively. Also shown is the charge gap, E_G, defined as $E_G = E(2N+1)+E(2N-1)-2E(2N)$, where $E(2N)$ is the ground state energy of a system with $2N$ electron. In the limit of infinite chains this will correspond to the energy of an uncorrelated particle-hole pair, as demonstrated by the fact that its energy extrapolates to ca. 3.2 eV, in agreement with the energies of the $m^1A_g^+$ and $n^1B_u^-$ states [19]. Our result for the band threshold agrees with an SCI calculation on a re-parametrised P-P-P model by Shimoi and Abe [2]. These considerations of the energetics and mean separation of the low lying states lead us to deduce that there are bands of both $^1B_u^-$ and $^1A_g^+$ excitons below the conduction band threshold.

The spatial correlation function, $C_{ij}(|n\rangle)$, may also be used to calculate the total weight of single-particle excitations in a given excited state compared to the ground state, defined as:

$$W(|n\rangle) = \sum_{i\,j} C_{ij}^2(|n\rangle) \tag{4}$$

Fig. 4 shows the single-particle weight for the most important singlet excited states. For the $^1B_u^-$ states there is no substantial difference between the excitonic and unbound states; both of them have a single-particle weight of about 0.75 for the longest oligomers studied. In contrast, the $^1A_g^+$ states show different values and behaviour of $W(|n\rangle)$ as a function of N. The share of the single-particle excitations in the lowest unbound $m^1A_g^+$ state increases as the oligomer size increases, approaching the values of the $^1B_u^-$ states. For the excitonic $2^1A_g^+$ state, however, the single-particle weight remains approximately constant, at about 0.28, independent of the system size. The small value of $W(|n\rangle)$ for the $2^1A_g^+$ state is consistent with the predominately triplet-triplet character of a strongly correlated state. The same values of about 0.1-0.3 were found for other excitonic states of $^1A_g^+$ symmetry.

3.2 The Triplet Spectrum

Photomodulation and photoinduced absorption probes of PPV have revealed the positions of the low-energy triplet excitations. The lowest $^3B_u^-$ state was found at 1.4 eV [20] and the triplet-triplet excitation at 1.45 eV [20] or 1.4 eV [21], thus giving the energy of the lowest $^3A_g^+$ state at 2.80-2.85 eV. The results of our calculation of the lowest triplet excitations are shown in Fig. 5. For the system with 14 phenylene rings

Figure 4: Single-particle weight of the key lowest bound and band states as a function of the number of phenylene units. $1^1B_u^-$ (solid diamonds), $n^1B_u^-$ (open diamonds), $2^1A_g^+$ (solid squares), $m^1A_g^+$ (open squares).

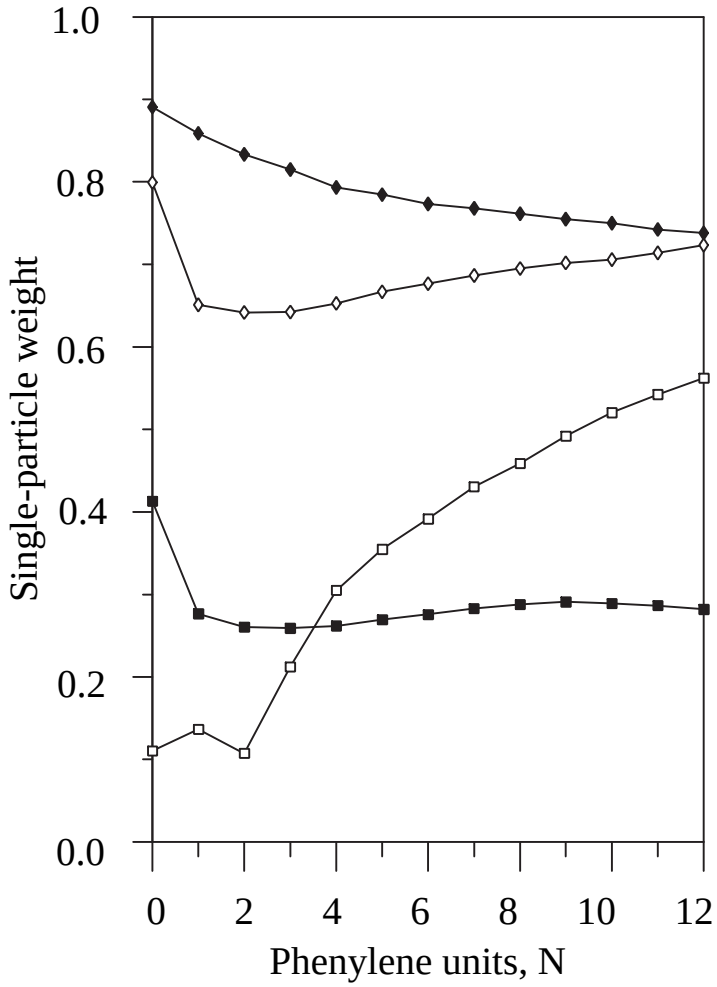

the energy of the ${}^3B_u^-$ state is 1.67 eV, while the energy of the ${}^3A_g^+$ state is 3.41 eV. A polynomial fit gives the energies of the ${}^3B_u^-$ and ${}^3A_g^+$ states at 1.64 eV and 3.27 eV, respectively, and 1.63 eV for the transition between them, in reasonable agreement with experiment.

Figure 5: The energies of the lowest triplet states, ${}^3B_u^-$ (solid diamonds) and ${}^3A_g^+$ (solid squares), as a function of the number of phenylene units.

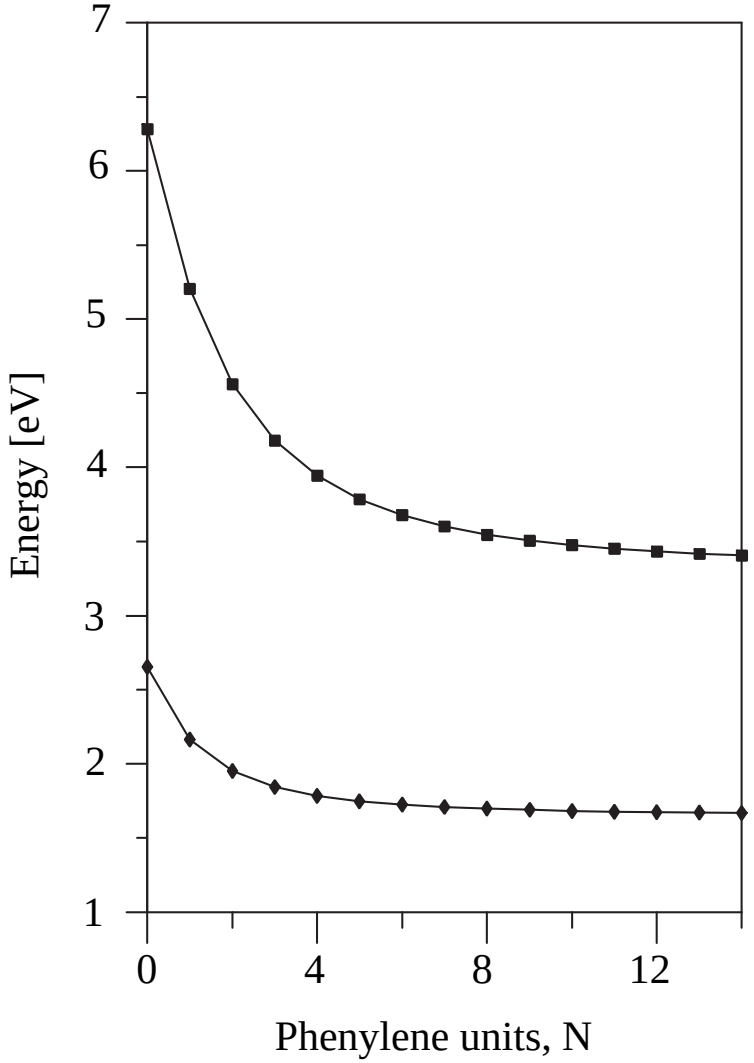

4 Optical Spectroscopies

Having calculated the energies, symmetries and spatial correlation functions of the low lying states a comparison to and interpretation of experiment can be made via the optical spectroscopies. The nonlinear optical properties of PPV can be related to the

third-order macroscopic susceptibility $\chi^{(3)}$ which, in turn, results from the third-order microscopic hyperpolarizability γ_{xxxx}:

$$\chi^{(3)}_{xxxx}(-\omega_\sigma;\omega_1,\omega_2,\omega_3) \propto \gamma_{xxxx}, \tag{5}$$

where $\omega_\sigma = \omega_1 + \omega_2 + \omega_3$. The calculation of γ_{xxxx} can be performed using the sum-over-states method (see, e.g., [22]):

$$\begin{aligned}\gamma_{xxxx}(-\omega_\sigma;\omega_1,\omega_2,\omega_3) = K(-\omega_\sigma;\omega_1,\omega_2,\omega_3)(-\hbar)^{-3}\\ I_{1,2,3}(\sum_{A,B,C}(\frac{\mu_{gA}\mu_{AB}\mu_{BC}\mu_{Cg}}{(\omega_A-\omega_\sigma)(\omega_B-\omega_1-\omega_2)(\omega_C-\omega_1)}+\frac{\mu_{gA}\mu_{AB}\mu_{BC}\mu_{Cg}}{(\omega_A^*+\omega_3)(\omega_B-\omega_1-\omega_2)(\omega_C-\omega_1)}+\\ \frac{\mu_{gA}\mu_{AB}\mu_{BC}\mu_{Cg}}{(\omega_A^*+\omega_1)(\omega_B^*+\omega_1+\omega_2)(\omega_C-\omega_3)}+\frac{\mu_{gA}\mu_{AB}\mu_{BC}\mu_{Cg}}{(\omega_A^*+\omega_1)(\omega_B^*+\omega_1+\omega_2)(\omega_C^*+\omega_\sigma)})-\\ \sum_{A,C}(\frac{\mu_{gA}\mu_{Ag}\mu_{gC}\mu_{Cg}}{(\omega_A-\omega_\sigma)(\omega_A-\omega_3)(\omega_C-\omega_1)}+\frac{\mu_{gA}\mu_{Ag}\mu_{gC}\mu_{Cg}}{(\omega_A-\omega_3)(\omega_C^*+\omega_2)(\omega_C-\omega_1)}+\\ \frac{\mu_{gA}\mu_{Ag}\mu_{gC}\mu_{Cg}}{(\omega_A^*+\omega_\sigma)(\omega_A^*+\omega_3)(\omega_C^*+\omega_1)}+\frac{\mu_{gA}\mu_{Ag}\mu_{gC}\mu_{Cg}}{(\omega_A^*+\omega_3)(\omega_C-\omega_2)(\omega_C^*+\omega_1)})),\end{aligned} \tag{6}$$

where μ_{ij} is the dipole matrix element for the transition between the states i and j, and $K(-\omega_\sigma;\omega_1,\omega_2,\omega_3)$ is a numerical constant which depends on the values of ω_σ, ω_1, ω_2, ω_3 [22]. $I_{1,2,3}$ denotes the average of all terms generated by permuting ω_1, ω_2 and ω_3. A finite lifewidth of the levels A, B, C should be taken into account in order to calculate γ_{xxxx} at the resonance points properly. In our calculations, the linewidth was taken to be 0.04 eV.

The sum in equation (6) is over all states. However, due to the fact that the ground state belongs to the $^1A_g^+$ symmetry sector, the dipole matrix elements are non-zero only for the transitions between $^1A_g^+$ and $^1B_u^-$. Thus, the states A and C in (6) are of $^1B_u^-$ symmetry, while the state B, as well as the ground state, are of $^1A_g^+$ symmetry.

4.1 Oscillator Strengths

The results for some of the most important transitions for oligomers of different sizes are given in Table 2. The transition with the largest oscillator strength is that between the ground state and the $1^1B_u^-$ exciton. Also, there is a large oscillator strength between the $1^1B_u^-$ exciton and the first unbound $^1A_g^+$ state, $m^1A_g^+$, as well as between the $2^1A_g^+$ exciton and the first unbound $^1B_u^-$ state, $n^1B_u^-$. The transitions between the excitonic, as well as between the unbound states have substantially smaller oscillator strength.

4.2 Two Photon Absorption

Fig. 6 shows the calculated TPA spectrum of a 10 phenylene unit oligomer. The weaker peak at 3.0 eV corresponds to the $2^1A_g^+$ state, while the stronger peak at 3.8

N	$1^1A_g^+ \rightarrow 1^1B_u^-$	$1^1B_u^- \rightarrow 2^1A_g^+$	$1^1B_u^- \rightarrow m^1A_g^+$	$2^1A_g^+ \rightarrow n^1B_u^-$	$m^1A_g^+ \rightarrow n^1B_u^-$
0	15.942 (4.17)	0.620 (1.07)	0.134 (5.34)	16.644 (3.01)	-3.500 (-1.27)
1	28.326 (3.52)	0.400 (0.54)	0.389 (2.68)	29.284 (2.48)	0.935 (0.33)
2	39.612 (3.18)	0.733 (0.38)	7.985 (2.01)	40.196 (2.02)	2.771 (0.38)
3	49.898 (2.99)	1.225 (0.32)	49.332 (1.68)	50.632 (1.68)	10.981 (0.32)
4	60.021 (2.88)	1.905 (0.30)	78.323 (1.51)	57.173 (1.42)	17.269 (0.22)
5	69.481 (2.80)	2.672 (0.30)	90.479 (1.39)	61.899 (1.24)	20.306 (0.15)
6	79.035 (2.76)	3.579 (0.30)	93.486 (1.30)	64.469 (1.09)	19.523 (0.09)
7	88.383 (2.73)	4.430 (0.30)	75.882 (1.23)	65.876 (0.98)	14.281 (0.05)
8	97.784 (2.72)	5.149 (0.31)	79.097 (1.18)	66.521 (0.89)	7.760 (0.02)
9	106.932 (2.70)	5.795 (0.32)	73.221 (1.14)	39.431 (0.84)	7.474 (0.02)
10	116.580 (2.70)	6.365 (0.32)	63.492 (1.10)	59.735 (0.77)	-7.971 (-0.01)
11	124.450 (2.70)	6.986 (0.32)	54.943 (1.07)	60.744 (0.73)	-17.293 (-0.02)

Table 2: Calculated oscillator strengths for selected transitions in oligophenylenes with different number of phenylene units, N. (The corresponding energy differences in eV are shown in brackets.)

Figure 6: The calculated TPA spectrum of a 10 phenylene unit oligomer.

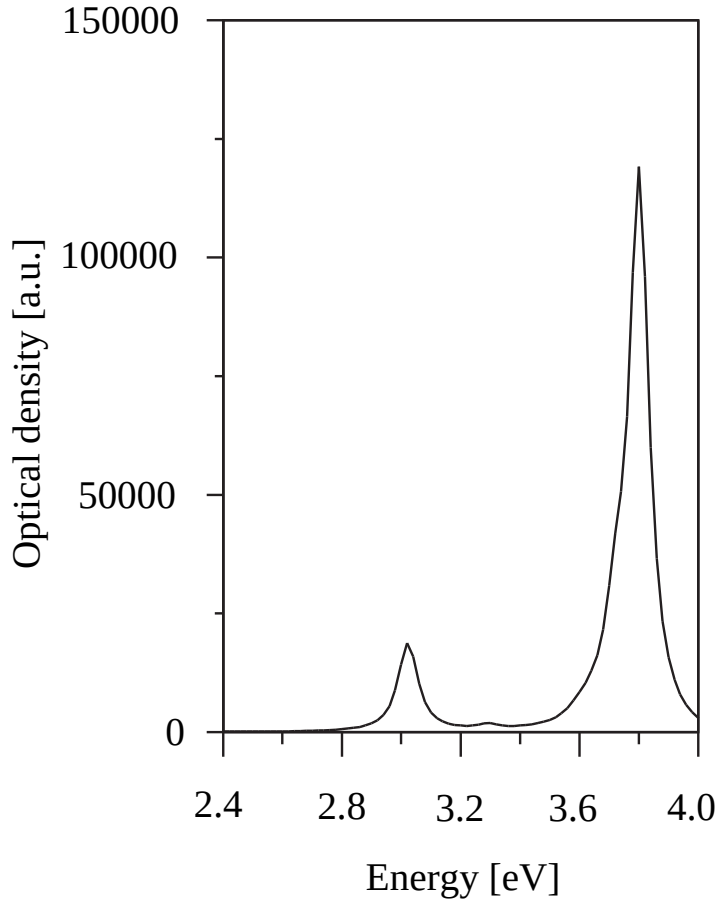

eV is the $m^1A_g^+$ state. Baker et al.[23] performed two photon fluorescence measurements on PPV. They observed a strong signal at 2.9 eV and a weak feature at 3.2 eV. An interpretation of the relative weights of these peaks is complicated, because instrumental sensitivity determines the strengths of the observed transitions. Long et al. [24] observed a weak low energy peak at ca. 3.0 eV, and evidence for a steep increase in absorption at ca. 3.2 eV. This sharp increase in the TPA at 3.2 eV has also been observed by Meyer et al. [25] in a derivative of PPV. We ascribe the low and high energy features observed in [23] and [24] to the $2^1A_g^+$ and $m^1A_g^+$ states, respectively, while we interpret the strong 3.3 eV absorption of [25] as the $m^1A_g^+$ state.

4.3 Electroabsorption

In order to take into account the vibronic structure of the EA spectra the sums in (6) are carried out over the vibrational levels $\omega_I + n\omega$ (where ω_I is the electronic state energy, n is an integer and ω is the energy of a phonon). The dipole moments are multiplied by the relevant Franck-Condon overlap factor, F_{pq}, which is given by [26, 27]

$$F_{pq}(a) = \frac{e^{-a^2/4}}{\sqrt{2^{p+q}p!q!}} \sum_r \frac{2^r(-1)^{q-r}a^{p+q-2r}p!q!}{r!(p-r)!(q-r)!}, \tag{7}$$

where p and q are the phonon levels between which the transition occurs, a is the difference in configurational coordinate between the two electronic states involved and the sum is up to the smaller of p or q. To simplify the calculation the same phonon energy was used for all the states.

The existence of a range of conjugation lengths within the polymer films results in the excited states existing over a range of energies. Further, since the nonlinear response is strongly dependent on the conjugation length, the longer segments within the distribution will contribute more to the overall response of the system than the shorter segments. Liess et al. [28] modeled this effect by introducing an asymmetric distribution function $\zeta(\omega')$ and calculated the function

$$\chi^{(3)}_{film}(-\omega;0,0,\omega) = \int_{-\delta}^{+\delta} \zeta(\omega')\chi^{(3)'}_{SOS}(-\omega;0,0,\omega)d\omega', \tag{8}$$

where ω' is the difference between energies of excited states in finite oligomer and infinite system, and the $\chi^{(3)'}_{SOS}$ is the sum-over-states susceptibility including vibronic effects, calculated with the energies $\omega_A, \omega_B, \omega_C$ increased by ω'. Near to resonances the measured EA signal is proportional to the imaginary part of the nonlinear susceptibility $\chi^{(3)}(-\omega;0,0,\omega)$. The lineshape calculated from (8) can thus be compared directly to the measured EA lineshapes.

The calculated EA spectrum of a 10 phenylene unit oligomer is shown in Fig. 7 (a). The three sharp peaks are the phonon-split derivative-like feature corresponding to the red-shifted $1^1B_u^-$ exciton, while the maximum at ca. 3.8 eV corresponds to the conduction band threshold A_g^+ and B_u^- states. The weak feature below the $m^1A_g^+$

Figure 7: (a) The calculated EA spectrum of a 10 phenylene unit oligomer. (b) The experimental EA spectrum of a PPV thin film, from [17]

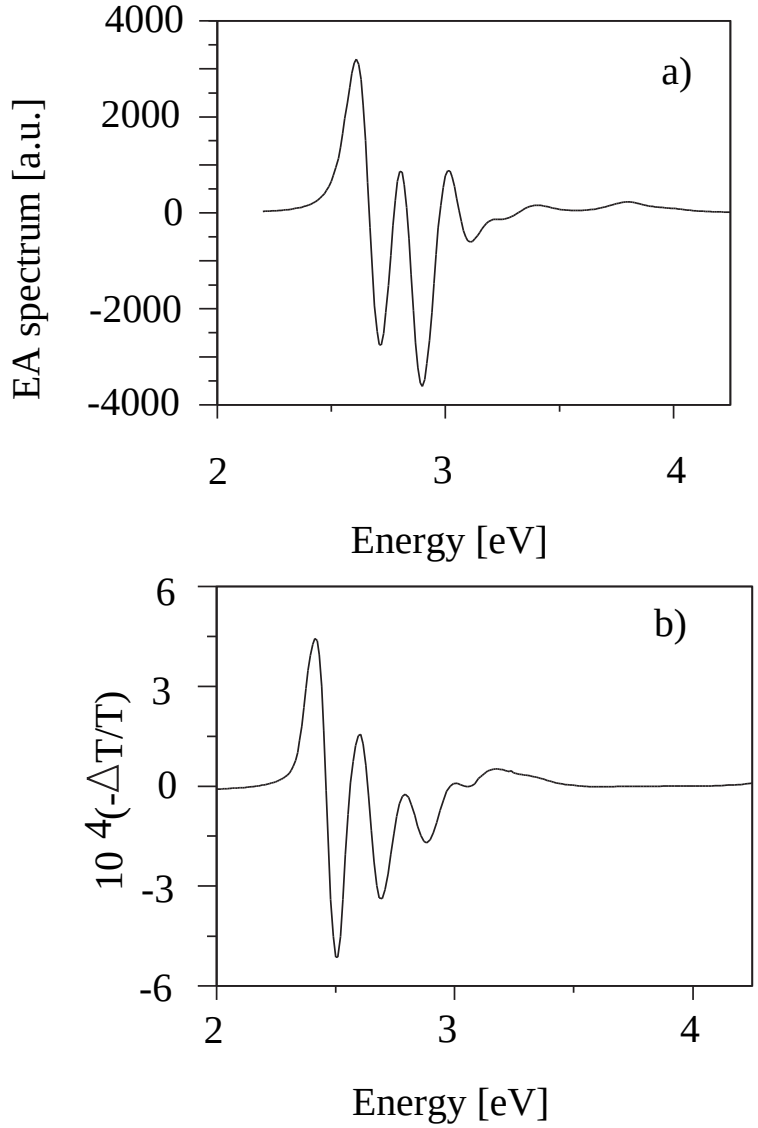

state is the $2^1A_g^+$ state. The experimental EA spectrum from [17] is shown in Fig. 7 (b). The broad maximum at 3.2 eV, with no correspondence in the derivative of the linear absorption, signifies an $^1A_g^+$ state. That this state is the band threshold $m^1A_g^+$ state is confirmed by the TPA spectrum discussed above, the observation of a $^1B_u^-$ state (namely the $n^1B_u^-$ state) at the same energy by THG [29] and the onset of photo-conductivity at ca. 3.2 eV [30]. It is most likely that the $2^1A_g^+$ state, observed in the TPA, has been obscured either by the vibronic structure of the $1^1B_u^-$ exciton, or by the $m^1A_g^+$ state (which is at a lower energy than the theoretical calculation).

5 Discussion and Conclusions

The parametrised 2-MO model of the phenyl based semiconductors predicts bands of $^1B_u^-$ ('s'-wave excitons) and $^1A_g^+$ ('p'-wave excitons) below the conduction band threshold. The $1^1B_u^-$ exciton energies are in close agreement with oligomer and thin film results. The experimental two-photon fluorescence [23] and TPA [24] lends support to there being an excitonic $^1A_g^+$ state at ca. 2.9 eV.

The conduction band threshold states have been identified by their mean particle-hole spacing, and by the fact that their energies approach the charge gap. These states have strong transition dipole moments to the low lying excitonic states and thus contribute strongly to the non-linear optical spectroscopies, i.e. TPA and EA. A comparison of the calculated EA and TPA spectra with the measured spectra strongly suggests that the conduction band threshold states lie at ca. 3.2 eV in PPV thin films. This result is confirmed by the observation of a $^1B_u^-$ state by THG, and is consistent with photo-conductivity experiments.

The experimental thin film band threshold of 3.2 eV lies lower than the theoretical prediction of 3.8 eV for a 10 phenylene unit oligomer. The reasons for this are two fold. First, the conjugation length in thin films may be somewhat larger than 10 phenylene units, so an energy tending towards the infinite polymer result of 3.2 eV could be expected. Second, and more importantly, as shown by Moore and Yaron [31], the theoretical single chain predictions of the band threshold states have less relevance to thin films than do the predictions of the excitonic states, because the band states are more subject to the polarisation effects of the surrounding medium. Moore and Yaron considered a model system of a solvent polyene chain of 24 atoms and a solute polyene chain of between 2 and 18 carbon atoms, separated by $4\mathring{A}$. Solving the P-P-P model, they found that the B_u^- exciton was solvated by 0.06 eV, while the charge-gap was solvated by 0.38 eV, leading to a reduction in the binding energy of 0.32 eV. In [32] this calculation was extended to 18 solvent chains. Taking the thermodynamic limit, they predicted a reduction of the binding energy of 1.3 eV. Such a large reduction may not be applicable to PPV, but fairly large solvation energies are expected.

The interpretation that the band threshold is at 3.2 eV gives an experimental estimate of the energy differences between the vertical energies of the $1^1B_u^-$ and $2^1A_g^+$ excitons and the band gap as ca. 0.4 eV and 0.2 eV, respectively. The difference in

energy between the relaxed $1^1B_u^-$ state (at 2.4 eV) and the band gap is 0.8 eV.

Our calculated $1^1B_u^-$ exciton binding energy, ranging from ca 0.9 eV for a 13 phenylene unit oligomer to ca. 0.6 eV for infinite chains, is almost certainly an over-estimate of the true binding energy. The multi-chain solute-solvent calculation discussed above [31], [32] suggests that it is at least 0.3 eV too high.

Shimoi and Abe [2] and Chandross and Mazumdar [3] both predicted a binding energy of 0.9 eV for a single chain. Again, solid-state solvation is expected to decrease this value. The phenomenological model by Gartstein, Rice and Conwell [6] gives binding energy between 0.2 and 0.4 eV, depending on the parameter set. The semiconductor band calculation of Gomes da Costa and Conwell [4], which incorporates three-dimensional effects, predicted a binding energy of 0.4 eV. The calculation of Beljonne et al. [7] is reasonably consistent with ours. They also used a two band model to describe the low energy excitations. However, the parameters are obtained directly from an INDO Hamiltonian, and the model is solved for oligomers of up to 6 phenyl(ene) rings using MRD-CI. Their predictions of the $1^1B_u^-$ at 3.13 eV, the $2^1A_g^+$ at 3.78 eV, the $m^1A_g^+$ at 4.28 eV and the $n^1B_u^-$ state at 4.73 eV for an eight phenylene oligomer, are similiar to ours, although somewhat blue shifted. They also interpret the $n^1B_u^-$ state as the band threshold state.

The lowest triplet state is calculated to be at ca. 1.6 eV, with the triplet-triplet gap being ca. 1.6 eV. These predictions are in reasonable agreement with the experimental results [20], [21].

It is instructive to compare the results of this calculation to our earlier calculation on PPP [10] and to P-P-P model calculations on polyacetylene (PA) [33] [34]. PPV, being composed of phenylene and vinylene repeat units is, in a sense, a hybrid of PPP and PA. The PPP calculation predicts only a band of ${}^1B_u^-$ excitons, with the $2^1A_g^+$ state representing the band threshold. In contrast, most calculations predict that in PA the vertical energy of the $2^1A_g^+$ state lies below the $1^1B_u^-$ [34]. The PPV calculation lies intermediate to both of these, with both ${}^1B_u^-$ and ${}^1A_g^+$ excitons. Thus, the vinylene unit behaves as a more highly correlated unit than the phenylene unit.

In conclusion, we have presented theoretical evidence for the existence of B_u^- and A_g^+ excitons in PPV. The theoretical calculation was based on the suitably parametrised two-state model of conjugated semiconductors. Our interpretation of the experimental non-linear spectroscopies, in the light of our theoretical calculation, leads to an estimate of energy difference of ca. 0.4 eV between the vertical energy of the $1^1B_u^-$ exciton and the band gap and ca. 0.8 eV between the relaxed energy of the $1^1B_u^-$ exciton and the band gap. This is consistent with other experimental predictions [35], [36].

Acknowledgments

We thank Dr. D. Beljonne (Mons), Prof. D. D. C. Bradley (Sheffield), Dr. C. Castleton (Grenoble) and Prof. D. Yaron (Carnegie-Mellon) for useful discussions. M. Yu. L. and S. J. M. are supported by the EPSRC, grants GR/K86343 and GR/L84209, respectively. H. D. is supported by an EPSRC studentship. R.J.B. is supported by the Australian Research Council.

*On leave from Institute of Inorganic Chemistry, 630090 Novosibirsk, Russia

References

[1] Burroughes, J. H., Bradley, D. D. C., Brown, A. R., Marks, R. N., Mackay, K., Friend, R. H., Burn, P. L., and Holmes, A. B., Light emitting diodes based on conjugated polymers. Nature **347**, 539 (1990).

[2] Shimoi, Y. and Abe, S., Electronic and optical properties of neutral and charged poly(p-phenylene vinylene). Synth. Met. **78**, 219 (1996).

[3] Chandross, M. and Mazumdar, S., Coulomb interactions and linear, nonlinear, and triplet absorption in poly(para-phenylenevinylene). Phys. Rev. **B 55**, 1497 (1997).

[4] Gomes da Costa, P. and Conwell, E. W., Excitons and the band gap in poly(phenylene vinylene). Phys. Rev. **B 48**, 1993 (1993).

[5] Rice, M. J. and Gartstein, Yu. N., Excitons and interband excitations in conducting polymers based on phenylene. Phys. Rev. Lett. **73**, 2504 (1994).

[6] Gartstein, Yu. N. Rice, M. J., and Conwell, E. M., Electron-hole interaction effects in the absorption spectra of phenylene-based conjugated polymers. Phys. Rev. **B 52**, 1683 (1995).

[7] Beljonne, D., Cornil, J., dos Santos, D. A., and Bredas, J. L., A molecular description of the nonlinear optical response in poly(paraphenylene vinylene), manuscript in preparation.

[8] Harigaya, K., Excitons in the optical absorption spectra of the electroluminescent polymer poly(para-phenylenevinylene). J. Phys.: Condens. Matter **9**, 5253 (1997); Optical excitations in electroluminescent polymers: the poly(paraphenylenevinylene family). J. Phys.: Condens. Matter **9**, 5989 (1997).

[9] Barford, W. and Bursill, R. J., The Theory of Molecular Excitons in the Phenyl-based Organic Semiconductors. Chem. Phys. Lett. **268**, 535 (1997).

[10] Barford, W., Bursill, R. J. and Lavrentiev, M. Y., Density matrix renormalisation group calculations of the low-lying excitations and non-linear optical properties of poly(p-phenylene). J. Phys.: Condens. Matt., **10** 6429 (1998).

[11] White, S. R., Density-matrix algorithms for quantum renormalisation groups. Phys. Rev. **B 48**, 10345 (1993).

[12] Bursill, R. J., Barford, W. and Daly, H., Molecular Orbital Models of Benzene, Biphenyl and the Oligophenylene, To appear in Chemical Physics.

[13] Bursill, R. J., Castleton, C. and Barford, W., Optimal Parameterisation of the Pariser-Parr-Pople Model for Benzene and Biphenyl, Chem. Phys. Lett. **294**, 305 (1998).

[14] Castleton, C. and Barford, W., Optimal Parameterisation of the Pariser-Parr-Pople model for Benzene, Biphenyl and trans-stilbene, proceedings of ICSM98.

[15] The full P-P-P model calculation of stilbene predicts a $^1A_g^+$ state at 4.39 eV. However, this is derived from the B_{3g} state, and is not described by the 2-MO model [14].

[16] Woo, H. S., et al., Optical Spectra and Excitations in poly(p-phenylene vinylene). Synth. Met. **59** 13 (1993).

[17] Martin, S. J., Mellor, H., Bradley, D. D. C., and Burn, P. L., Electroabsorption studies of PPV and MEH-PPV. Opt. Materials, **9**, 88 (1998).

[18] Dixit, S. N., Guo, D. and Mazumdar, S., Essential states mechanism of optical nonlinearity in π conjugated polymers. Phys. Rev. **B 43**, 6781 (1991).

[19] We believe that the exact agreement between the infinite single chain result and the experimental data on thin films of shorter conjugation length (see §4) for the band threshold energy is largely coincidental.

[20] Leng, J. M., Jeglinski, S., Wei, X., Benner, R. E., Vardeny, Z. V., Guo, F. and Mazumdar, S., Optical probes of Excited States in poly(p-phenylenevinylene). Phys. Rev. Lett. **72**, 156 (1994).

[21] Pichler, K., Halliday, D. A., Bradley, D. D. C., Burn, P. L., Friend, R. H. and Holmes, A. B., Optical spectroscopy of highly ordered poly(p-phenylenevinylene). J. Phys.: Condens. Matter **5**, 7155 (1993).

[22] Orr, B. J. and Ward, J. F., Perturbation theory of the non-linear optical polarization of an isolated system. Mol. Phys. **20**, 513 (1971).

[23] Baker, C. J., Gelsen, O. M., and Bradley, D. D. C., Location of the lowest even parity singlet state in PPV by two-photon fluorescence spectroscopy. Chem. Phys. Lett. **201** 127 (1993).

[24] Long, X., unpublished data.

[25] Meyer, R. K., Benner, R.E., Vardeny, Z.V., Liess, M., Ozaki, M., Yoshino, K., Ding, Y. and Barton, T., Two-Photon Absorption Spectra of Luminescent Conducting Polymers. Synth. Met. **85**, 549 (1997).

[26] Soos, Z. G. and Mukhopadhyay, D., Vibronic analysis of overlapping resonances and the third-harmonic-generation spectrum of β-carotene. J. Chem. Phys. **101**, 5515 (1994).

[27] Mukhopadhyay, D., and Soos, Z. G., Nonlinear-optical and electroabsorption spectra of polydiacetylene crystals and films. J. Chem. Phys. **104**, 1600 (1996).

[28] Liess, M., Jeglinski, S., Vardeny, Z. V., Ozaki, M., Yoshino, K., Ding, Y., and Barton, T., Electroabsorption spectroscopy of luminescent and nonluminescent π-conjugated polymers. Phys. Rev. B **56**, 15712 (1997).

[29] Mathy, A., Ueberhofen, K., Schenk, R., Gregorius, H., Garay, R., Mullen, K., and Bubeck, C., Third-harmonic-generation spectroscopy of poly(p-phenylene vinylene): A comparison with oligomers and scaling laws for conjugated polymers. Phys. Rev. **B 53**, 4367 (1996).

[30] Chandross, M., Mazumdar, S., Jeglinski, S., Wei, X., Vardeny, Z. V., Kwock, E. W. and Miller, T. M., Excitons in poly(para-phenylene vinylene). Phys. Rev. **B50**, 14702 (1994).

[31] Moore, E., and Yaron, D., Models of Coulomb screening and exciton binding in conjugated polymers. Synth. Met. **85**, 1023 (1997).

[32] Moore, E., and Yaron, D., An explicit-solvent dynamic-dielectric screening model of electron-hole interactions in conjugated polymers. J. Chem. Phys. **109**, 6147 (1998).

[33] Boman, M. and Bursill, R. J., Identification of excitons in conjugated polymers: A density matrix renormalisation group study. Phys. Rev. B **57**, 15167 (1998).

[34] Lavrentiev, M. and Barford, W, The $1^1B_u^- - 2^1A_g^+$ crossover in one-dimensional chains: The phase diagram of the molecular orbital model. Submitted (1998).

[35] Kersting, R., Lemmer, U., Deussen, M., Bakker, H.J., Mahrt, R.F., Kurz, H., Arkhipov, V.I., Bassler, H., and Gobel, E.O., Ultrafast Field-Induced Dissociation of Excitons in Conjugated Polymers. Phys. Rev. Lett. **73**, 1440 (1994).

[36] Marks, R.N., Halls, J.J.M., Bradley, D.D.C., Friend, R.H., and Holmes, A.B., The photovoltaic response in poly(p-phenylene vinylene) thin film devices. J. Phys. Condens. Matter **6**, 1379 (1994).